Role of surface and bulk plasmon decay in secondary electron emission

Wolfgang S. M. Werner,[1,*] Alessandro Ruocco,[2] Francesco Offi,[2] Stefano Iacobucci,[3] Werner Smekal,[1] Hannspeter Winter,[1] and Giovanni Stefani[2]

[1]*Institut für Allgemeine Physik, Vienna University of Technology, Wiedner Hauptstraße 8-10, A 1040 Vienna, Austria*

[2]*Dipartimento di Fisica e Unità CNISM, Università di Roma Tre, via della Vasca Navale 84, I-00146 Rome, Italy*

[3]*CNR-Istituto Sistemi Complessi, Area della Ricerca di Roma 1, Via Salaria km 29.300, 00016 Monterotondo, Italy and Unità CNISM, Università di Roma Tre, via della Vasca Navale 84, I-00146 Rome, Italy*

(Received 5 November 2008; published 8 December 2008)

The mechanism of secondary electron emission by impact of 100-eV electrons on an Al(100) surface has been investigated by measuring the secondary electron spectrum in coincidence with loss features in the spectrum of reflected electrons. Distinct peaks are observed at energies corresponding accurately to the surface and bulk plasmon energies minus the work function of the analyzer, demonstrating that plasmons excited by electron energy losses predominantly decay via creation of single-electron-hole pairs that act as a source for the secondary electron spectrum. These findings suggest a mechanism for emission of secondary electrons very similar to photoelectron (PE) emission, the difference being the step leading to electron liberation, i.e., plasmon decay in the present case versus photoionization in the case of PE.

DOI: 10.1103/PhysRevB.78.233403 PACS number(s): 78.20.Ci, 68.49.Jk, 79.20.Uv

Emission of secondary electrons (SE) is of importance in many branches of fundamental and applied science. It is widely employed in the electron microscope for the investigation of the structure and electronic state of solid surfaces[1] and particle detection in electron multiplier devices, and generally it is related to the energy dissipation of energetic particles moving inside a solid.[2] Low-energy SE may dramatically affect high-energy physics accelerators and storage rings where photoelectrons produced by synchrotron radiation can lead to emission of SE and the creation and evolution of the electron cloud causes beam instability.[3,4] Detailed understanding concerning the SE emission mechanism is also of importance for the plasma-wall interaction in a fusion reactor since SE emitted from the surface of the vessel containing the plasma govern the plasma stability to an important degree.[5] SE emission also plays a crucial role in the energy and charge balance of gaseous electronics such as plasma display panels.[6,7]

Progress in the fields addressed above hinges on an improved understanding of the SE emission mechanism, which can then be taken into account in the modeling of these phenomena. Unfortunately, SE emission is still far from being quantitatively understood, and experimental data for the SE yield exhibit a large scatter in some cases exceeding a factor of 7.[8] The lack of quantitative understanding concerning SE emission is partly due to the experimental difficulty to separate the generation inside the solid, transport to the surface and escape from the latter, and the fact that the SE cascade cannot be resolved experimentally. From the theoretical point of view, it is generally accepted that plasmon decay plays an essential role in the SE production mechanism,[9–11] but the only evidence for the contribution of plasmon decay to SE emission seems to be the (weak) features in the derivative of the SE spectrum,[9,12] which are not very well suited for a detailed investigation of the phenomenon. Such features are also observed in spectra of ion-induced electrons.[13] Coincidence measurements between the energy-loss spectrum of the primary electrons and the secondary spectrum can be used to get a more detailed insight into the role of plasmon decay in SE emission. Several authors have employed this technique in a transmission electron microscope.[14–18] Evidence for a contribution of surface excitations to secondary electron emission was found in some of these works, in particular for the aloof geometry measurements on MgO_2, but the energy distribution of the secondary electrons emitted as a result of surface and bulk plasmon decay could not be clearly resolved.

It should be emphasized at this stage that the decay of plasmons *per se* (in particular surface plasmons) is also receiving increasing attention recently since it is of paramount importance for subwavelength optical components explored in the fields of plasmonics and nanophotonics.[19,20] Since plasmon decay puts a limit on the propagation length of surface plasmons, it is highly relevant for the development of plasmonic devices such as field-enhancing elements,[21] surface-enhanced Raman spectroscopy, devices coupling surface plasmons to light,[22] waveguides,[23] mirrors,[24] and splitters.[25] Sometimes, the decay of surface plasmons is a desired effect, as in the surface-plasmon-assisted laser cooling of solids.[26]

In the present work, the relationship between plasmon decay and emission of SEs is investigated. The plasmon decay is monitored by measuring the SE spectrum in coincidence with the features corresponding to the excitation of surface and bulk plasmons in the energy-loss spectrum. Analysis of the coincidence spectrum demonstrates that plasmons excited by electron energy losses decay predominantly via creation of single-electron-hole pairs that act as a source for the SE spectrum, in analogy to the photoelectron emission process.

The experimental setup is schematically illustrated in Fig. 1. Two hemispherical analyzers (flanged to the vacuum chamber with base pressure 5×10^{-10} mbar) are used to record the energy-loss spectrum and the SE spectrum with a polar opening angle of $\pm0.5°$ and $\pm2°$ and an effective energy resolution of 1.0 and 1.2 eV, respectively. The work function ϕ_A of the carbon-coated analyzer collecting the SE was determined by measuring the Fermi edge of a spectrum

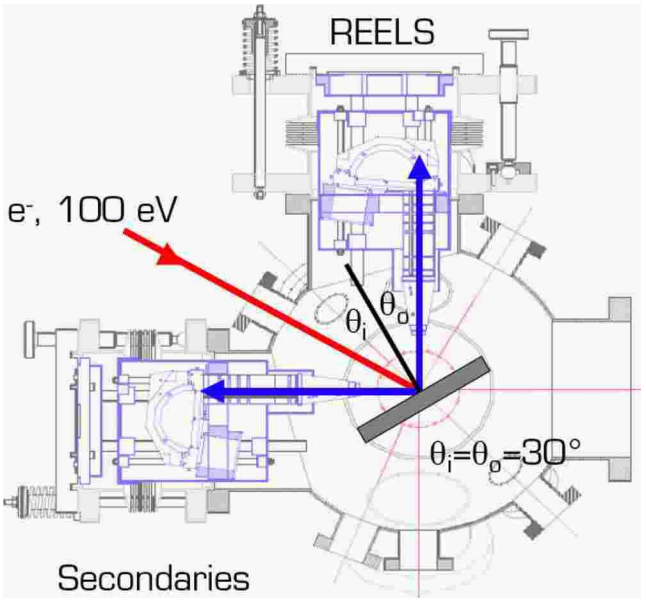

FIG. 1. (Color online) Schematic illustration of the experimental setup showing the incoming beam of primary electrons that strike the Al(100) target under an angle of 30° (off normal), the SE detector, as well as the analyzer for the energy-loss spectrum. The scattering geometry for the reflected beam is exactly specular with an incoming and outgoing direction of 30°.

excited by a glow discharge lamp and was found to be (4.3 ± 0.1) eV. Coincidences are detected by conventional electronics that consist of a preamplifier, a constant fraction discriminator, and a delay for each channel. The scattered electron triggers a start pulse; the stop signal is provided by the secondary electron. The timing signals are fed to a time to amplitude converter whose output is processed by an analog-to-digital converter directly connected to the PC bus. The time spectra recorded in this way exhibit a peak of true coincidences.

The experimental geometry is indicated in Fig. 1. By monitoring the elastic peak intensity, which exhibits a sharp maximum at the Bragg condition, the specular reflection geometry was aligned for all measurements with an accuracy of the order of 0.1°. The whole apparatus is located within a large Helmholtz cage which compensates the earth magnetic field. An Al(100) specimen was mounted in the sample holder and cleaned by repeated cycles of Ar^+-ion bombardment until clear diffracted beams could be observed with low energy electron diffraction (LEED). This cleaning procedure was repeated every 24 h and subsequently acquisition of coincidences was started. The intensity of the primary beam was adjusted to equalize the rates of true and false coincidences within the time-resolving window. Typical true coincidence count rates, which are mainly determined by the acceptance angle of the analyzers, were below 5×10^{-3} Hz under these conditions. Two SE spectra were scanned ($2 \leq E \leq 15$ eV) in coincidence with an energy loss corresponding to the surface and bulk plasmon.

Figure 2 displays reflection electron energy loss spectroscopy (REELS) spectra of the single-crystal Al(100) surface. The surface (10.5 eV, blue arrow) and volume (14.9 eV, red

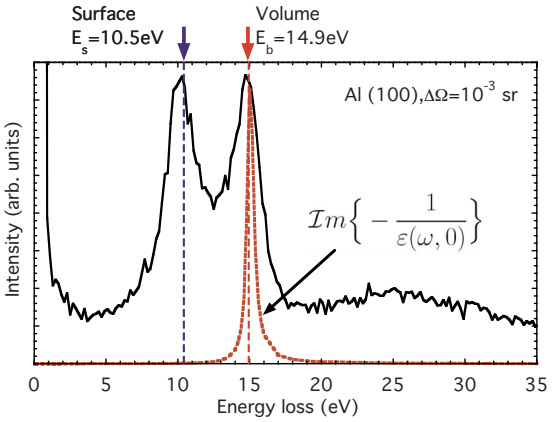

FIG. 2. (Color online) Energy-loss spectrum of 100-eV electrons reflected from a single-crystal Al(100) surface compared with the energy-loss function for zero momentum transfer (Ref. 29).

arrow) plasmon loss features in the single-crystal spectrum are very pronounced and sharp. The volume plasmon is seen to compare well with the energy-loss function at zero momentum transfer, $\mathrm{Im}\{-1/\varepsilon(\omega,0)\}$. This is consistent with the kinematics of the experiment that corresponds to a momentum transfer close to zero in a specular-reflection geometry.[27] Therefore, also the plasmon created in this process has a momentum close to zero.

In Fig. 3, the SE spectrum (bold green curve) is compared with the SE spectrum in coincidence with the surface (blue diamonds) and bulk plasmon (red circles) loss. For these measurements, the analyzer detecting the scattered electrons was set to the energy of the bulk (14.9 eV) and surface (10.5 eV) plasmons, respectively, while the other analyzer was scanned through the SE spectrum. The black solid curves

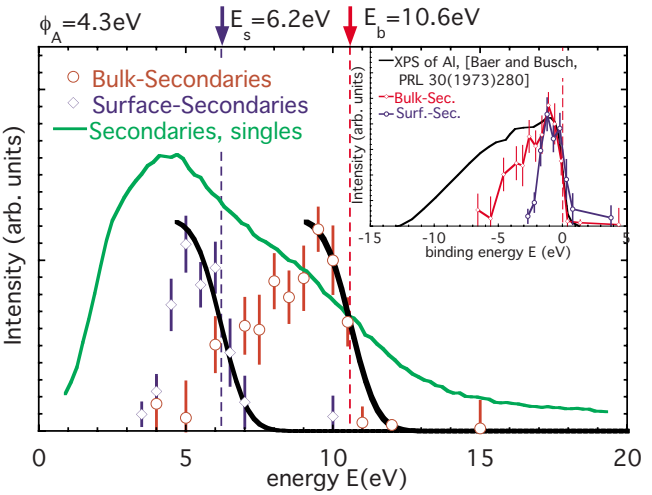

FIG. 3. (Color online) Data points with error bars: experimental SE spectra measured in coincidence with the surface (diamonds, blue) and volume (circles, red) loss features in the REELS spectra. The solid black curves represent the Fermi distribution broadened by the experimental energy resolution. The solid (green) curve is the single SE spectrum. The inset compares the (shifted) coincidence spectra with the valence-band XPS spectrum of a polycrystalline Al-film by Baer and Busch (Ref. 32).

represent the Fermi distribution broadened by the experimental energy resolution at energies corresponding to the surface and volume plasmon energy minus the analyzer work function. These curves accurately match the high-energy onset of the coincidence spectra. The ordinate scale is in arbitrary units, but the scale for the two coincidence spectra is the same. The SE spectrum exhibits a peak at ~5 eV and a shoulder at ~10 eV, which has been tentatively attributed to volume plasmon decay in the past.[9,12,13]

The fact that the onset of the coincidence spectra accurately matches the surface and volume plasmon energy losses shifted by the analyzer work function allows a clear identification of the peaks in the coincidence spectra as SE emitted as a result of surface and volume plasmon decays. The agreement of the energy of the peak in the bulk plasmon secondary-coincidence spectrum with the shoulder in the singles SE spectrum at about 10 eV, as well as the existence of a peak corresponding to surface plasmon decay, provides direct experimental proof of earlier conjectures concerning the role of surface and bulk plasmon decays in SE emission on the basis of derivative singles SE spectra.[9,13] In our experiment, the magnitude of the contribution of surface and volume plasmon decays is comparable, but it should be kept in mind that the measurement of secondaries in coincidence with the bulk and surface loss features in the loss spectrum (indicated by the blue and red arrows in Fig. 2) selects two very special types of trajectories, i.e., those electrons that are *reflected* before or after experiencing a *single* surface or volume plasmon loss,[27] while the majority of secondaries are expected to be produced by primaries that have lost a larger fraction of their energy *irrespective* of the fact that they are eventually reflected from the surface or not. Furthermore, the primary energy employed in our experiment is quite low (E_0=100 eV), which is favorable for surface plasmon excitation. Nonetheless, in earlier high-energy experiments on C and Si,[14–16,28] the surface loss features are also clearly visible in the *singles* spectra and are of similar relative magnitude as in the present loss spectra. The fact that these earlier experiments do not show any trace of *coincidences* between the surface losses and the SE spectrum is not understood.

The energy balance and the sharp distribution of coincidence electron spectra suggest that the plasmon excited by the primary electron decays in a single-electron-hole pair. Other processes that involve more than one electron or a phonon should be less favorable;[30] besides, they should lead to a continuous distribution that is not observed in our spectra. As previously stated, in our experiment the momentum of plasmons is approximately equal to zero. The decay of these plasmons gives rise to a vertical interband transition of a bound electron close to the Fermi level of the solid; intraband transitions involving other particles such as a second electron or a phonon are forbidden by momentum conservation.

The kinematics in our experiment is also compatible with an impact ionization process,[31] where an incident electron transfers part of its energy and momentum to a bound electron that is emitted. The plasmon creation and subsequent decay can be interpreted as a resonant channel for the direct impact ionization. Indeed, when the energy lost by the primary electron is resonant with a plasmon excitation, both channels, impact and plasmon decays, share identical initial and final states. To verify the predominance of the resonance channel over the direct impact channel, the SE spectrum was measured in coincidence with the loss spectrum 5 eV above the bulk plasmon energy. This led to a dramatic drop in the coincidence yield. In other words, direct impact ionization is not ruled out but its relative intensity is much smaller than the resonant plasmon excitation.

The shape of the coincidence spectra is related to the intrinsic width of the plasmon, the energy resolution of the experiment, and the band structure of aluminum. The steep descent observable in the high-kinetic-energy side in the case of the bulk plasmon is connected with the emission of electrons from the Fermi level in analogy to photoemission (in our experiment the role of the photon is played by the plasmon). This interpretation is confirmed by the agreement between the high-energy onset of the coincidence spectra and the black solid curves (see Fig. 3) that represent the Fermi distribution broadened by the experimental energy resolution. The inset of Fig. 3 compares the x-ray photoelectron spectrum (XPS) of a polycrystalline Al film[32] with the coincidence spectra shifted by 10.6 eV (volume) and 6.2 eV (surface). The position and the shape of the onset of the XPS spectrum of Ref. 32 are seen to match our data accurately, but the overall shape is different. The fact that the positions of the onsets match agrees with the theoretical prediction that plasmon decay at the present kinetic energies mainly proceeds via an interband transitions of single electrons[30] not assisted by another particle such as a phonon or a second electron. A quantitative interpretation of the difference of the shape of the spectra can only be established by comparing them with theoretical calculations. We note however that the differences between the XPS valence-band spectrum and our data is attributable to the fact that the XPS data were acquired on a polycrystalline sample with a high kinetic energy compared to our measurements. The XPS spectrum, thus, represent an average over the Brillouin zone, while our measurements are more momentum selective and should yield sharper peaks, as indeed observed in the inset of Fig. 3.

The differences between the surface and bulk coincidence spectra are believed to be related to the difference in dispersion of the surface and the bulk plasmon. Furthermore, for the considered trajectories, bulk plasmon excitation takes place over a depth region comparable to the SE escape depth of the order of several nanometers, while the width of the surface scattering zone at low energies is much smaller, implying that the surface plasmon decay mainly samples the surface band structure, which may be essentially different from the volume band structure sampled by the volume plasmon. Finally, the small width of the peaks in the coincidence spectra suggests that the cascade of higher-order secondaries is not strongly pronounced for the (special) type of trajectories discriminated by our experiment. The cascade is also expected to be different for surface and bulk plasmon decay.

In conclusion, we have studied the mechanism of SE emission by monitoring the decay of surface and bulk plasmons via coincidence measurements of the electron energy-loss spectrum with the SE spectrum. Sharp peaks at energies corresponding to the surface and bulk plasmon energies provide direct and unambiguous proof of the fact that surface

and bulk plasmon decays lead to emission of SE. Together with the shape of the SE energy distribution this leads us to propose that observed SEs are emitted via a mechanism very similar to photoelectron emission when plasmon decay plays the role of photon absorption.

Support by the Austrian Science Foundation FWF (Project No. P20891-N20) and MIUR, Italy (PRIN 2005 Grant No. 2005021433) is gratefully acknowledged. We are indebted to A. Rizzo and G. Di Filippo for their assistance during the experiment.

*werner@iap.tuwien.ac.at

[1] L. Reimer, *Scanning Electron Microscopy* (Springer-Verlag, Berlin, 1985).
[2] M. Kimura, M. Inokuti, and M. A. Dillon, Adv. Chem. Phys. **84**, 193 (1993).
[3] R. Cimino, I. R. Collins, M. A. Furman, M. Pivi, F. Ruggiero, G. Rumolo, and F. Zimmermann, Phys. Rev. Lett. **93**, 014801 (2004).
[4] K. Ohmi, Phys. Rev. Lett. **75**, 1526 (1995).
[5] G. Fubiani, H. P. L. de Esch, A. Simonin, and R. S. Hemsworth, Phys. Rev. ST Accel. Beams **11**, 014202 (2008).
[6] T. J. Vink, A. R. Balkenende, R. G. F. A. Verbeek, H. A. M. van Hal, and S. T. de Zwart, Appl. Phys. Lett. **80**, 2216 (2002).
[7] H. S. Uhm, E. H. Choi, and G. S. Cho, Appl. Phys. Lett. **78**, 592 (2001).
[8] Y. Lin and D. C. Joy, Surf. Interface Anal. **37**, 895 (2005).
[9] M. S. Chung and T. E. Everhart, Phys. Rev. B **15**, 4699 (1977).
[10] J. P. Ganachaud and M. Cailler, Surf. Sci. **83**, 498 (1979).
[11] M. Rösler and W. Brauer, Phys. Status Solidi A **104**, 161 (1981).
[12] C. V. von Koch, Phys. Rev. Lett. **25**, 792 (1970).
[13] R. A. Baragiola and C. A. Dukes, Phys. Rev. Lett. **76**, 2547 (1996).
[14] D. Voreades, Surf. Sci. **60**, 325 (1976).
[15] F. J. Pijper and P. Kruit, Phys. Rev. B **44**, 9192 (1991).
[16] H. Müllejans and A. L. Bleloch, Phys. Rev. B **46**, 8597 (1992).
[17] H. Müllejans, A. L. Bleloch, A. Howie, and M. Tomita, Ultramicroscopy **52**, 360 (1993).
[18] H. Müllejans, A. L. Bleloch, A. Howie, and C. A. Walsh, Philos. Mag. Lett. **68**, 145 (1993).
[19] T. W. Ebbesen, H. J. Lezec, H. F. Ghaemi, T. Thio, and P. A. Wolff, Nature (London) **391**, 667 (1998).
[20] J. M. Pitarke, V. M. Silkin, E. V. Chulkov, and P. M. Echenique, Rep. Prog. Phys. **70**, 1 (2007).
[21] B. Sepúlveda, A. Calle, L. M. Lechuga, and G. Armelles, Opt. Lett. **31**, 1085 (2006).
[22] H. Ditlbacher, J. R. Krenn, A. Hohenau, A. Leitner, and F. R. Aussenegg, Appl. Phys. Lett. **83**, 3665 (2003).
[23] B. Steinberger, A. Hohenau, H. Ditlbacher, A. L. Stepanov, A. Drezet, F. R. Aussenegg, A. Leitner, and J. R. Krenn, Appl. Phys. Lett. **88**, 094104 (2006).
[24] M. U. Gonzalez, J.-C. Weeber, A.-L. Baudrion, A. Dereux, A. L. Stepanov, J. R. Krenn, E. Devaux, and T. W. Ebbesen, Phys. Rev. B **73**, 155416 (2006).
[25] H. Ditlbacher, J. R. Krenn, G. Schider, A. Leitner, and F. R. Aussenegg, Appl. Phys. Lett. **81**, 1762 (2002).
[26] J. B. Khurgin, Phys. Rev. Lett. **98**, 177401 (2007).
[27] A. Ruocco, M. Milani, S. Nannarone, and G. Stefani, Phys. Rev. B **59**, 13359 (1999).
[28] J. Drucker, M. R. Scheinfein, J. Liu, and J. Weiss, J. Appl. Phys. **74**, 7329 (1993).
[29] E. D. Palik, *Handbook of Optical Constants of Solids* (Academic, New York, 1985).
[30] G. A. Bocan and J. E. Miraglia, Phys. Rev. A **72**, 042903 (2005).
[31] A. Liscio, A. Ruocco, G. Stefani, and S. Iacobucci, Phys. Rev. B **77**, 085116 (2008).
[32] Y. Baer and G. Busch, Phys. Rev. Lett. **30**, 280 (1973).